



Research Article



Long-term rainfall projection based on CMIP6 scenarios for Kurau River Basin of rice-growing irrigation scheme, Malaysia

Muhammad Nasir Mohd Adib^{1,2}  · Sobri Harun¹ · Md. Kamal Rowshon²

Received: 21 October 2021 / Accepted: 13 January 2022

Published online: 05 February 2022

© The Author(s) 2022 [OPEN](#)

Abstract

Rainfall is a vital component in the rice water demand model for estimating irrigation requirements. Information on how the future patterns are likely to evolve is essential for rice-growing management. This study presents possible changes in the future monthly rainfall patterns by perturbing model parameters of a stochastic rainfall using the change factor method for the Kerian rice irrigation scheme in Malaysia. An ensemble of five Global Climate Models under three Shared Socioeconomic Pathways (SSPs) (SSP1-2.6, SSP2-4.5, and SSP5-8.5) were employed to project rainfall from 2021 to 2080. The results show that the stochastic rainfall generator performed well at preserving the statistical properties between simulated and observed rainfall. Most scenarios predict the increasing trend of the mean monthly rainfall with only a few months decreasing in April and May occurring in off (dry) season. The future patterns 2051–2080 show a significant increasing trend during main (wet) season compared to the near future period (2021–2050). The projected future rainfall under SSP1-2.6 and SSP2-4.5 are higher than SSP5-8.5 from January to July, and December but lower from August to November. The projected annual rainfall will significantly increase toward 2080 during the main-season but uniform during the off-season except under SSP5-8.5, which is significantly decreasing. The output results are essential for rice farmers and water managers to manage and secure future rice irrigation water under the impact of future climate change. The projected changes in rainfall on the river basin demand further study before concluding the impact consequences for the rice sector.

Article highlights

- The rainfall generator performs well in simulating future rainfall based on an ensemble of five different GCMs considering three different scenarios emission (low, medium, and high) caused by greenhouse gas and radiative forcing.
- The future rainfall projection predicted that off (dry) season would become wet, and main (wet) season would become wetter due increase in monthly and annual rainfall.
- The outcomes of this paper are beneficial for rice farmers and water managers of the study area to manage their rice cultivation and water release from the reservoir schedules to avoid losses due to flood and drought.

Keywords Rainfall generator model · Kurau River Basin · Climate change · CMIP6 · Shared socioeconomic pathways

✉ Muhammad Nasir Mohd Adib, adibnasir_89@yahoo.com | ¹School of Civil Engineering, Universiti Teknologi Malaysia, 81310 UTM Johor Bahru, Johor, Malaysia. ²Department of Biological and Agricultural Engineering, Universiti Putra Malaysia, 43400 UPM Serdang, Selangor, Malaysia.



SN Applied Sciences

(2022) 4:70

| <https://doi.org/10.1007/s42452-022-04952-x>

1 Introduction

Malaysia experiences hot and humid weather throughout the year, named equatorial climate. The Southwest and the Northeast Monsoons cause climate variability, occurring in April to September and October to March. The Southwest Monsoon features drier weather, while Northeast Monsoon has abundant rainfall [1]. However, in the last two decades, Malaysia has faced warming and rainfall irregularities [2]. Climate change in Malaysia is mainly related to surface air temperature, sea surface temperature, sea level, and precipitation [3, 4]. Kurau River Basin, with an area of approximately 322 km² located in the north of Peninsular Malaysia, is a dominant upstream part of the Bukit Merah Reservoir catchment [5], where it is the primary irrigation source for large scale Kerian rice irrigation scheme. The Asia region is the leading rice producer with approximately 94% of the world's production, consuming over 90% of the total irrigation supply from river basins [6, 7]. The uncertain rainfall pattern in rice cultivation will produce a complex way for operators to predict and plan the irrigation demand for the coming month if the climate is inconsistent. More than 51% of rice water requirements of massive rice fields are primarily fulfilled by rainfall with wet-season (February–July) practicing supplemental irrigation while dry-season (August–January) practicing full irrigation [8]. Although Malaysia is blessed with rainfall all year round, there is still an unanswered question about water availability coupled with climate change's impact on rice cultivation in this area.

One step forward to face the climate forcing challenges is through the projection of future rainfall scenarios. Global climate models (GCMs) developed by many organizations with Coupled Model Intercomparison Project (CMIP) are the progressive and advanced data to assess future challenges [9]. The current version of CMIP is CMIP6 is an ensemble of CMIP-endorsed Model Intercomparison Projects (MIPs) that provides an extensive version compared to CMIP5 in terms of the number of models and releases scenarios [10]. GCMs under CMIP6 differ from CMIP5 in three general ways such as higher horizontal resolution, more complexity of physical scheme of models, and new shared socio pathways (SSPs) scenarios replacing representative concentration pathways (RCPs) [11–14]. In the latest most advanced structure of CMIP6, the SSP scenarios are advanced in energy, land use, and uncertainty related to greenhouse gases and emissions compared to RCPs scenarios [15]. Specifically, CMIP6 simulation seeks to broaden the understanding of three raised questions: how the earth system reacts to climate change signals, what are the

origins and consequences of systematic model biases, and how future climate forcings can be assessed based on the scenarios narratives [16].

Average conditions of hydro-meteorological parameters are always considered in crop cultivation [8, 17], unlike when dealing with flood assessment where the extreme event is crucial to be analyzed [10]. Therefore, the selection of downscaling technique plays a vital role in the analysis considering the different focus areas and time scales of climate change impact assessment. Weather generators are stochastic models under statistical methods used for generating hydro-meteorological parameters for local-scale by referring to historical data series as a baseline [18]. The stochastic nature of the model is receiving attention in water resources-related applications such as agriculture to generate long daily synthetic data as input parameters [17, 19]. Weather generator models have evolved, adapting with the GCM models as climate change related studies and relatively inexpensive and less time-consuming [20]. Two types of weather generator models are parametric models and semi-parametric models. Richardson weather generator (WGEN) is one of parametric models based on Markov-chain dependent and distribution function for simulating rainfall occurrence and rainfall amount, respectively [20, 21]. In comparison, Semenov and Barrow (1997) developed semi-parametric models that applied semi-empirical distributions to simulate rainfall processes. Details for further review on their history and previous successful application can be found from Wilby [22], Dlamini et al. [8], Fadhil et al. [23], and Liu et al. [24].

Several studies have implemented the CMIP models, especially CMIP5, in projecting future rainfall in different parts of Malaysia. Dlamini et al. [8] and Adib et al. [25] examine 10 CMIP5 models for future rainfall projection in the Northwest and North part of Peninsular Malaysia, respectively. Their results indicated a similar pattern, in which most GCMs predicted a decreasing trend in future rainfall from January to February and an increase from July to December. Tan et al. [26] used 17 ensemble models under CMIP5 to forecast future rainfall patterns in the Southern part of Malaysia, and the result indicated a clear increase pattern during Southwest Monsoon and decreased pattern during Northwest Monsoon periods. Hussain et al. [27] conducted a study at Sarawak of Borneo Island, Malaysia, to assess the future rainfall changes using CanESM5 of the CMIP5 model. The model reveals that Sarawak will experience lesser rainfall during December to February period and more during June to August. In another study using the latest CMIP model, Tan et al. [28] assessed rainfall patterns in the Kelantan river basin, the northeast part of Peninsular Malaysia, using CMIP6 HighResMIP Experiments. The study showed that monthly rainfall is projected to increase during the Southwest

Monsoon (June–September) and the early phase of the Northeast Monsoon (December), and the remaining months experienced a decreasing pattern. All the result showed that most of the region in Peninsular Malaysia seem to have similar monthly future rainfall patterns yet the pattern slightly different from Borneo Island, Malaysia. Based on the literatures, very few study in climate change assessment conducted in Malaysia region apply the CMIP6 models, accordingly emerging necessities to understand the impact of future climate change using this models.

This study aims to assess the future rainfall pattern considering climate change in the Kurau River Basin, which is the main water source for the Kerian rice irrigation scheme in the northern part of Malaysia. The ensemble of five GCMs of CMIP6 under three SSP scenarios (SSP1-2.6, SSP2-4.5, and SSP5-8.5) are used to reveal the rainfall pattern over the selected river basin from 2021 to 2080 based on GHG emission and radiative forcing level. The study applied the delta change factor method for perturbing rainfall generator parameters in downscaling the GCMs to the local scale for impact assessment. This paper analyzes the rainfall pattern for two planting seasons of the

rice scheme. The first planting season is from August to January, also known as main-season (wet-season), and the second planting season is from February to July, known as off-season (dry-season). Understanding the patterns of future rainfall characteristics is crucial for water resource management for the rice field, which always deals with a huge amount of water supply to cope with water stress during dry-season.

2 Materials and methods

2.1 Study area

The study area, Kurau River Basin, with a total area of 322 km², is located at the northern of Perak in Peninsular Malaysia within latitude 4°51'~5°10'N and longitude 100°38'~101°55'E as shown in Fig. 1. Kurau River Basin is a dominant upstream part of the Bukit Merah Reservoir catchment [5], where its headwork is integrated with Kerian rice irrigation scheme to satisfy the irrigation demands and cope with water shortages. It has a humid

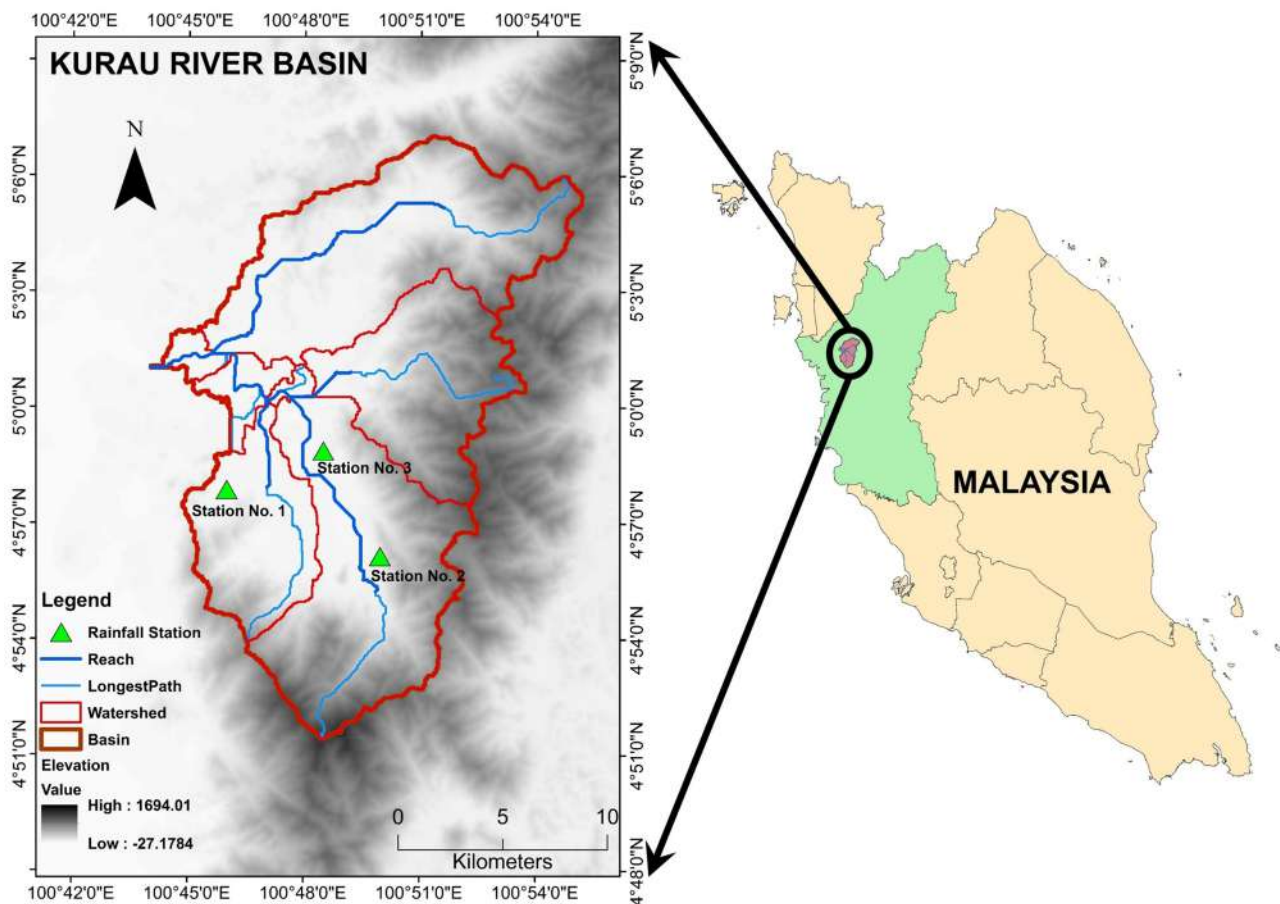


Fig. 1 Location of Kurau River Basin Malaysia and rainfall stations

Table 1 List of rainfall stations

Station no.	Station name	Latitude	Longitude
4907019	Ladang Norseman	4°57'55"	100°45'50"
4908013	Ibu Bekalan Sempeneh di Batu Kurau	4°56'05"	100°49'40"
4908018	Pusat Kesihatan Kecil di Batu Kurau	4°58'45"	100°48'15"

Table 2 List of selected GCMs under CMIP6

No.	Model name	Country	Atmospheric resolution		Key references
			Lat	Lon	
1	CanESM5	Canada	2.8	2.8	Swart et al. [32]
2	MPI-ESM1-2-LR	Germany	1.9	1.9	Mauritsen et al. [33]
3	MRI-ESM2-0	Japan	1.1	1.1	Yukimoto et al. [34]
4	NESM3	China	1.9	1.9	Cao et al. [35]
5	NorESM2-LM	Norway	1.9	2.5	Seland et al. [36]

tropical climate which experiences an average temperature of about 27–28 °C with total annual rainfall of around 2500 mm [29]. The climate is influenced by two monsoon seasons: Southwest monsoon (May to August), which is considered the rainy season, and Northeast monsoon (November to February). Heavy rainfalls in the form of thunderstorms are expected during two inter-monsoon months, from March to April and from September to October, which causes intense convective rainfall to the western coast of Peninsular Malaysia [30, 31].

2.2 Data

2.2.1 Observations

In order to simulate rainfall at Kurau River Basin, daily rainfall is obtained from the Department of Irrigation and Drainage (DID) of Malaysia. Table 1 shows a list of rainfall stations chosen for the study area. The data selected are within the study area due to the availability and suitability of the data for coupling with a stochastic rainfall generator [23]. The period of data used in this study is from 1976 to 2005 to validate rainfall from the CMIP6 model (historical period).

2.2.2 CMIP6 models and scenarios

This study used precipitation data of CMIP6 models for the first realization ('r1i1p1f1') for five GCMs (CanESM5, MPI-ESM1-2-LR, MR-ESM2-0, NESM3, NorESM2-LM) (Table 2). The

GCMs are selected based on the availability of the required SSP scenarios under the first realization (r1i1p1f1). Three shared socioeconomic pathways (SSPs) scenarios, including SSP1-2.6, SSP2-4.5, and SSP5-8.5 scenarios used, represent low, medium, and high emission scenarios, respectively. The selected three ssp scenarios are appropriate to represent the level of emission scenario since rice fields are always associated with reference evapotranspiration mainly influenced by temperature. Details of summary regarding SSP narratives can be referred to Riahi et al. [14]. For analyzing the future rainfall, the future periods are segmented into 30 years' time period 2021–2050 (near future) and 2051–2080 (far future).

2.3 Modeling rainfall occurrence

Rainfall occurrence modeling based on a two-state Markov chain of first-order relies on whether the day is wet or dry and the probability of rain occurrence the previous day. This technique has performed well in many studies to generate synthetic rainfall [37–39]. This model is defined by the two transition probabilities, which are; (1) P_{01} , the probability of wet day proceeded by dry day, and (2) P_{11} , the probability of a wet day proceeded by another wet day, as expressed in Eqs. 1 and 2. These transitional probabilities are estimated from observed rainfall data.

$$P_{01} = P\{wet\ on\ day\ t | dry\ on\ day\ t - 1\} \tag{1}$$

$$P_{11} = P\{wet\ on\ day\ t | wet\ on\ day\ t - 1\} \tag{2}$$

A generated random numbers R_n between 0 to 1 are used to simulate rainfall occurrence $P_s(t)$. The value is then compared to the critical transition probability, P_c (Eq. 3), which relies on the rainfall state of the previous day where wet day = 1 and dry day = 0.

$$P_c = \begin{cases} P_{01} & \text{if } P_s(t - 1) = 1(wet) \\ P_{11} & \text{if } P_s(t - 1) = 0(dry) \end{cases} \tag{3}$$

Whenever the R_n is less or equal to the P_c , the rainy day will be simulated, or else, it is simulated as a dry day as stated in Eq. 4.

$$P_s(t) = \begin{cases} w & \text{if } R_n \leq P_c \\ d & \text{if } R_n > P_c \end{cases} \tag{4}$$

The other complementary probabilities for dry day following a dry day (P_{00}) and dry day following wet day (P_{10}) are related by Eqs. 5 and 6, respectively.

$$P_{00} = 1 - P_{01} \tag{5}$$

$$P_{10} = 1 - P_{11} \tag{6}$$

The transition probabilities for each station and month are computed as in Table 3.

The maximum likelihood estimation is used to determine transition probabilities for all months by employing Eq. 7 as

$$P_{ij} = \frac{N_{ij}}{N_t} \text{ for } i, j = 1, 2 \quad (7)$$

where N_t is N_0 when i is equal to 0, and N_t is N_1 when i is equal to 1.

2.4 Modeling rainfall amount

The amount of rainfalls on wet days is generated by employing the distribution function to get the mean rainfall per wet day. The gamma distribution has been used in this study because it is quite a synonym in rainfall modeling among researchers [37, 39, 40]. It is also the most appropriate and relevant method to model daily rainfall amount generation until today. The gamma distribution selects a threshold value of 1 mm for the Malaysia region due to high humidity conditions, as suggested by previous studies [29, 41]. Rainfall amount is then generated by sampling from two parameters of Gamma distribution. The probability density function (PDF) of the gamma distribution is given in Eq. 8 as

$$f(x) = \frac{\left(\frac{x}{\beta}\right)^{\alpha-1} \exp\left(-\frac{x}{\beta}\right)}{\beta\Gamma(\alpha)}; \quad \alpha, \beta > 0; \quad x > 0 \quad (8)$$

where $\Gamma(\alpha)$ is the gamma function, α and β are a shape and scale parameters, respectively. The maximum likelihood estimator is applied to compute the gamma parameters for each month to characterize the rainfall algorithm by four parameters (P_{01} , P_{11} , α , and β).

2.5 Perturbing rainfall generator parameters

The validated rainfall model is used to downscale GCMs outputs and simulates future rainfall series for each station in study area over Kurau River Basin. The model parameters are used to simulate future rainfall under climate scenarios (SSP1-2.6, SSP2-4.5, and SSP5-8.5) to be perturbing the derived observed rainfall parameter from GCM

outputs using the change factor method [8, 20, 42]. The change factors express the difference between the statics of the rainfall computed for the three scenario periods. Equation 9 represents the general approach adopted in change factors to calculate the ratio between statistical parameters for baseline and future periods [42] as

$$\frac{R^{FUT}}{R^{OBS}} = \frac{R^{GCM.FUT}}{R^{GCM.CTS}} \quad (9)$$

where R is the statistical property of rainfall, OBS and FUT represent observed and future rainfall scenarios, respectively, and GCM.CTS and GCM.FUT denote the GCM model generated for baseline and future scenarios, respectively.

2.6 Model verification

A site-specific rainfall modeling requires calibration and validation of statistical properties at each selected rainfall station. Daily observed rainfall data for 30 years (1976–2005) is used to evaluate the model performance. Estimating station representative parameters from generated daily series is done by running the model with 100 replications based on observed data to achieve reasonable generate statistical attributes that describe rainfall occurrence, quantity, and distribution, including monthly mean rainfall, standard deviation, rainy days, and wet and dry spells. The output from the rainfall model is then compared to the rainfall stations of the study area. Rainfall model performance is evaluated before it is applied for downscaling and future simulation to see how well the model preserves the statistical properties of the original data. Although this model generated daily rainfall series, the data analysis will use a monthly scale due to most crop cultivation practices considering average conditions of hydro-meteorological parameters.

3 Results and discussions

3.1 Stochastic rainfall generator model performance

Estimated transition probabilities and gamma parameters derived from the observed data indicate that during off (dry) season, the probability of rainfall to occur of the next day if the previous days not receiving rainfall is high. While, the chance of rainfall occurring when it is raining on the previous day is also high, and it increases during the main (wet) season of the rice planting period. Estimated transition probabilities of three rainfall stations for the observed period from 1976 to 2005 are shown in Table 4.

Table 3 Estimation of transition probabilities of observed rainfall

State of the day		Current day		Total (N_t)
		Dry (0)	Wet (1)	
Previous day	Dry (0)	N_{00}	N_{01}	N_0
	Wet (1)	N_{10}	N_{11}	N_1

Table 4 Estimation of transition probabilities of observed rainfall for different months and stations

Month	Jan	Feb	Mar	Apr	May	Jun	Jul	Aug	Sep	Oct	Nov	Dec
<i>Station 1 (4907019)</i>												
P_{00}	0.82	0.78	0.69	0.58	0.72	0.77	0.79	0.75	0.67	0.56	0.59	0.75
P_{10}	0.27	0.20	0.19	0.16	0.20	0.26	0.22	0.22	0.18	0.14	0.12	0.19
P_{01}	0.18	0.22	0.31	0.42	0.28	0.23	0.21	0.25	0.33	0.43	0.41	0.25
P_{11}	0.73	0.80	0.80	0.84	0.80	0.74	0.78	0.78	0.82	0.86	0.88	0.81
<i>Station 2 (4908013)</i>												
P_{00}	0.82	0.73	0.68	0.56	0.67	0.74	0.73	0.65	0.53	0.40	0.51	0.75
P_{10}	0.30	0.23	0.22	0.15	0.16	0.24	0.25	0.20	0.16	0.11	0.13	0.22
P_{01}	0.18	0.27	0.32	0.44	0.33	0.26	0.27	0.35	0.47	0.60	0.49	0.25
P_{11}	0.70	0.77	0.78	0.85	0.84	0.76	0.75	0.80	0.84	0.89	0.87	0.78
<i>Station 3 (4908018)</i>												
P_{00}	0.73	0.65	0.57	0.44	0.56	0.70	0.68	0.65	0.51	0.44	0.40	0.65
P_{10}	0.39	0.34	0.27	0.24	0.25	0.39	0.40	0.33	0.28	0.18	0.19	0.30
P_{01}	0.27	0.35	0.43	0.56	0.44	0.29	0.32	0.35	0.49	0.56	0.60	0.35
P_{11}	0.61	0.66	0.72	0.76	0.75	0.61	0.60	0.66	0.72	0.81	0.81	0.70

P_{01} =Probabilities for dry days followed by rain days; P_{00} =Probabilities for dry days followed by dry days; P_{10} =Probabilities for rain days followed by dry days; P_{11} =Probabilities for rain days followed by rain days

Figure 2 presents simulated total mean monthly rainfall and standard deviation for the observed period. It shows that the model is highly efficient in simulating mean daily rainfall with the R-squared value of 0.99 through all the months for all stations. High mean daily rainfall occurs during October and decreases gradually with a minimum value in January. A similar study on rainfall patterns in the

west region of Peninsular Malaysia also reported that peak rainfall occurs in April, May, and mid-August to late October, and the lowest mean rainfall occurs in late November to late February caused by the two inter-monsoon seasons [43, 44].

The model shows acceptable performance for standard deviation despite underestimating values for all

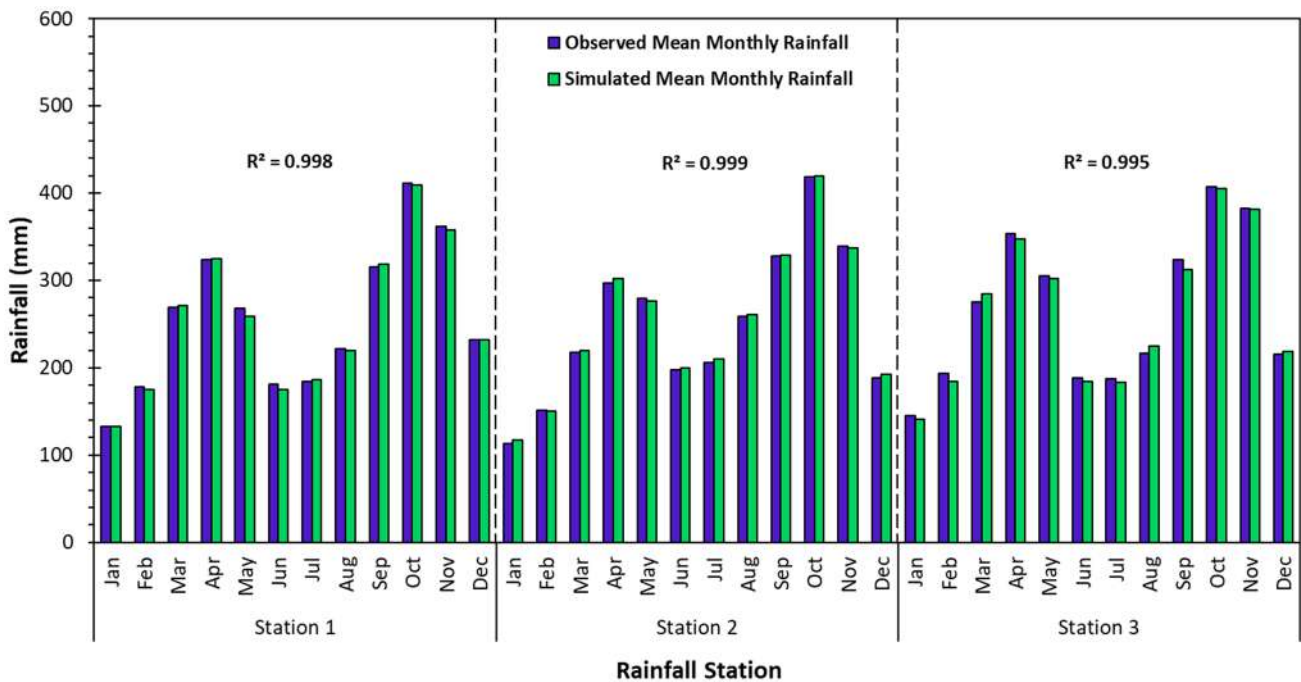


Fig. 2 Comparison of observed and model-simulated mean monthly rainfall at three stations

months except December for station 2 and March, August, and November for station 3 (Fig. 3), with the R-squared value of more than 0.95. Hence, indicating that the model has the ability to simulate rainfall patterns for the study area. It has also been reported that

most rainfall generator models have limitations in simulating rainfall variance [45].

Figure 4 shows a comparison of observed simulated wet and dry spells length where it is considered critical criteria for climate variability and climate change analysis, and

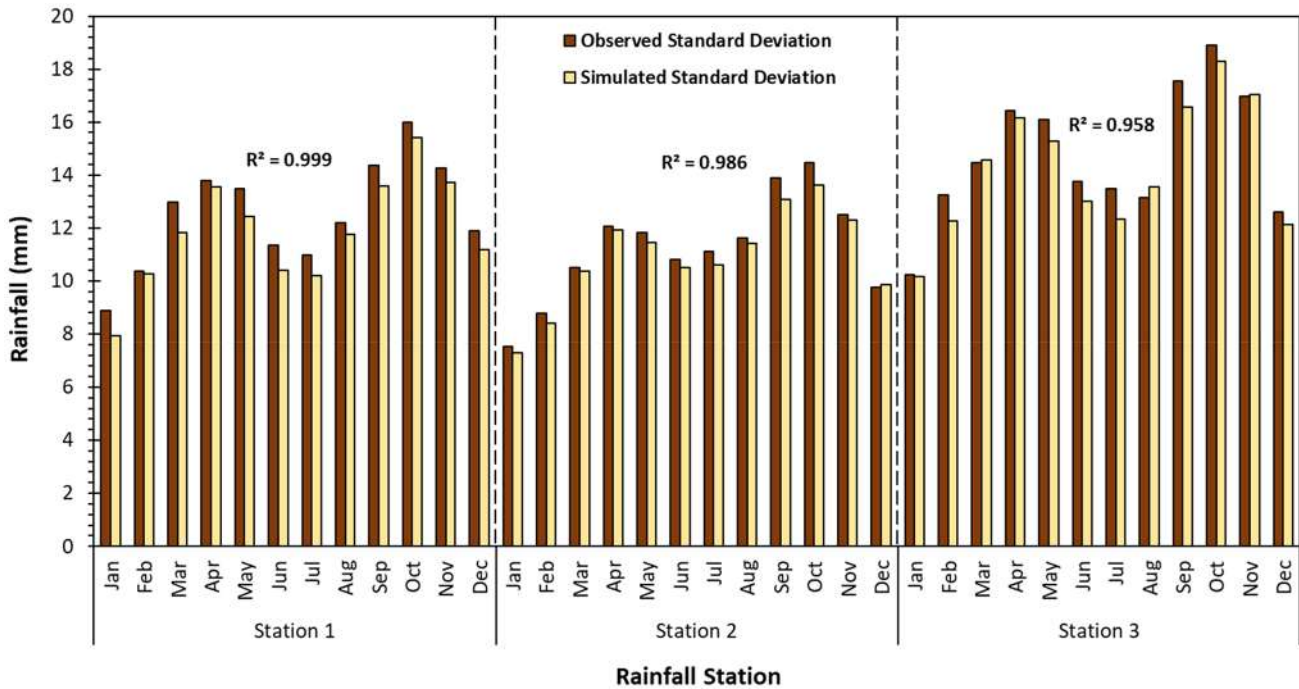


Fig. 3 Comparison of observed and model-simulated standard deviation at three stations

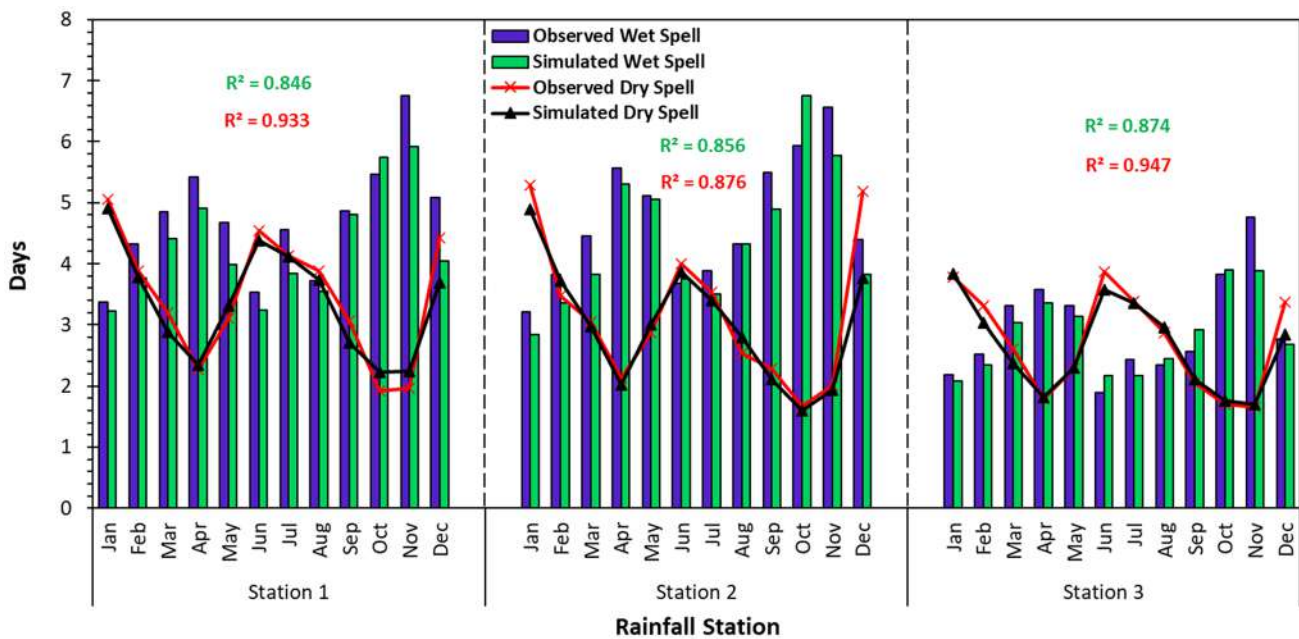


Fig. 4 Comparison of rainfall observed and simulated wet and dry spells for each station

water resources management. The model simulated both the wet spell and dry spell with R-squared values of more than 0.85. In detail, for the wet spell, the R-squared values are 0.846, 0.856, and 0.874 for station 1, station 2, and station 3, respectively. While for the dry spell, the R-squared values are 0.933, 0.876, and 0.947 for station 1, station 2, and station 3, respectively. The simulated dry spell shows more precise matches to the observed dry spell through all the months compared to the wet spell for all stations. The rainfall generator model proved to be able to simulate both wet and dry spell lengths excellently.

3.2 Projected changes in rainfall

The variability of downscaled individual CMIP6 models under SSP1-2.6, SSP2-4.5, SSP5-8.5, and multi-GCM ensemble for each scenario with recorded monthly rainfall for the period 2021–2080 can be observed in Fig. 5. The widespread in the selected climate models giving uncertainties prove the essential of implementation more than one

GCM in climate change study. As illustrated in Fig. 5, each GCM has its prediction representing a single projection of several future predictions. The projected mean monthly rainfalls are based on the CMIP6 multi-GCM simulations and three SSPs (SSP1-2.6, SSP2-4.5, and SSP5-8.5) for two future periods of 2021–2050 (near future) and 2051–2080 (far future) are illustrated in Fig. 6. The three SSP scenarios reveal an increasing trend of the future mean monthly rainfall during 2021–2050 and 2051–2080 except in April and May, which predicted decreasing trend of rainfall. Figure 7 illustrates the CMIP6 multi-GCM ensemble of projected changes by five GCMs with rainfall is predicted to be higher from July to December and January to March compared to the baseline period. It is more significant in February for the two future periods with a higher increment of 61.1% under SSP5-8.5 for the near future period and 60.2% under SSP2-4.5 for the far future period. While from April to June seem to be lower compared to the baseline period and more significant for April and May with a higher reduction of 14.5% under SSP5-8.5 for the near

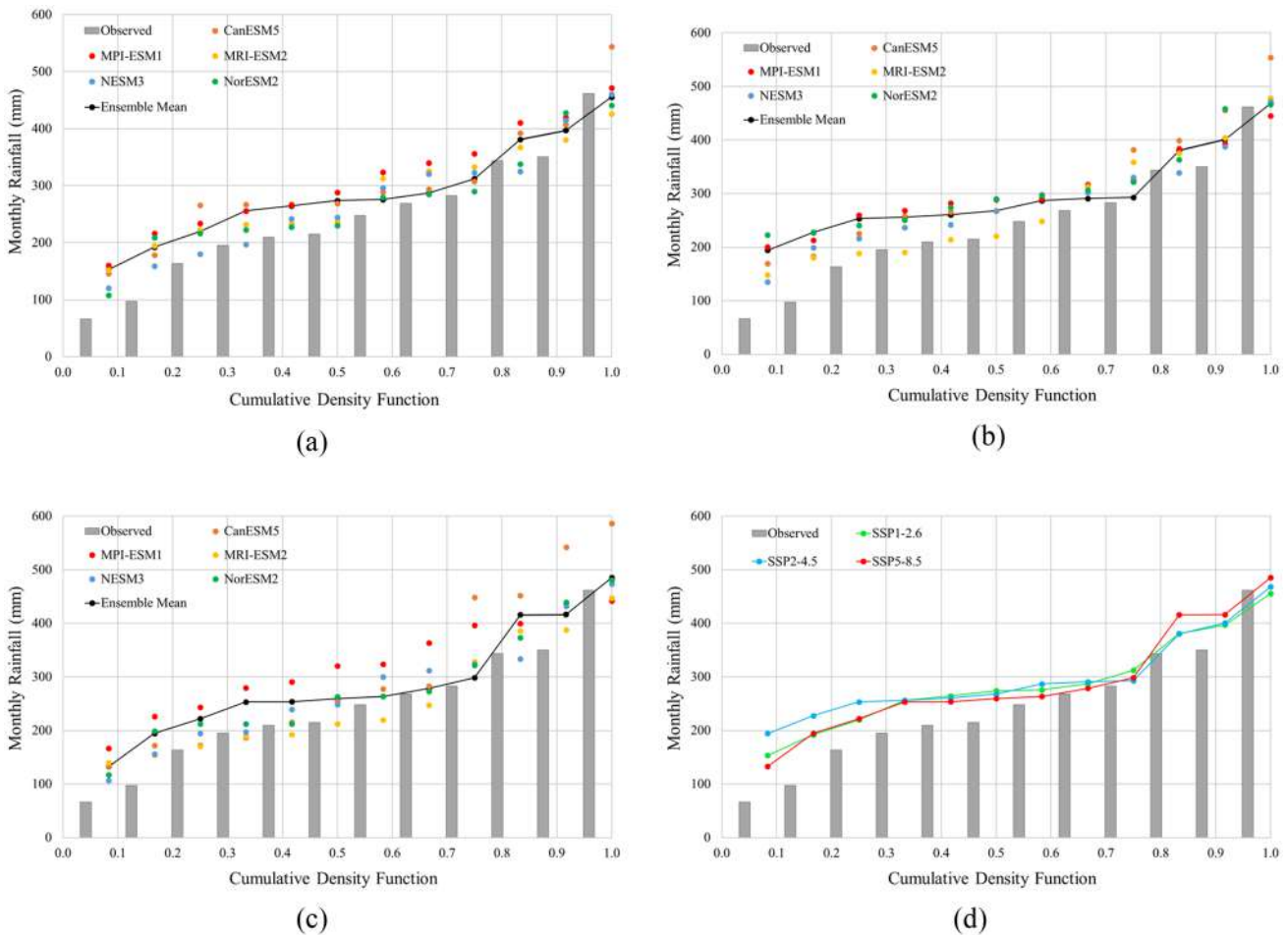


Fig. 5 Variability of downscaled individual CMIP6 model and multi-GCM ensemble under; **a** SSP1-2.6, **b** SSP2-4.5, **c** SSP5-8.5, and **d** multi-GCM ensemble for each scenario with recorded monthly rainfall

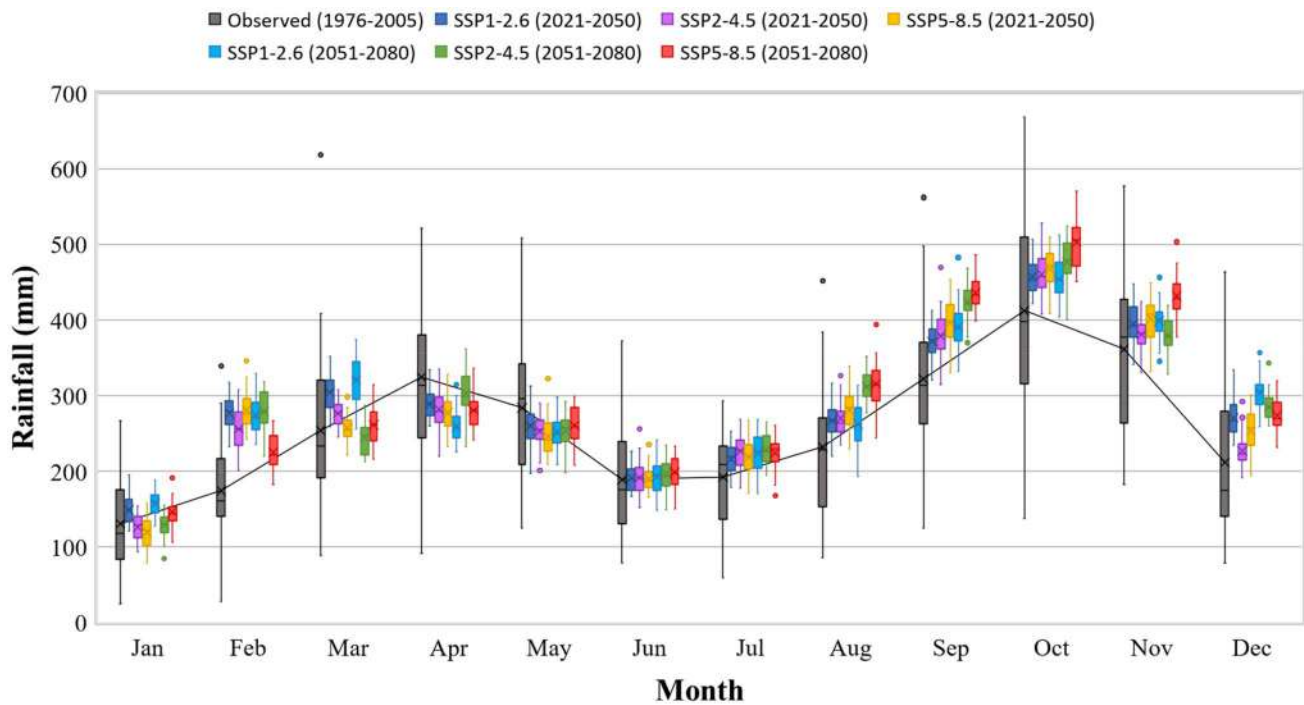


Fig. 6 Projected ensemble mean monthly rainfalls under SSP1-2.6, SSP2-4.5, and SSP5-8.5 scenarios for future periods 2021–2050 and 2051–2080 and with respect to baseline period of 1976–2005 with mean of baseline values (line)

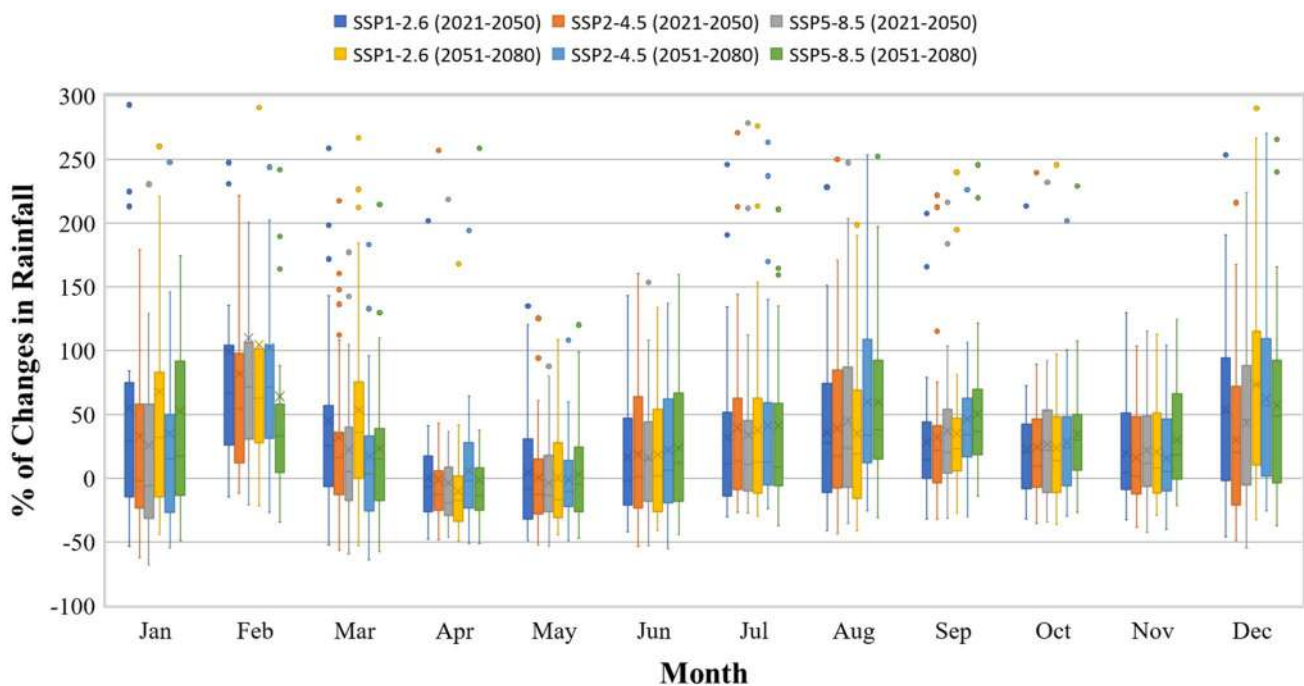


Fig. 7 Percent of changes of projected ensemble mean monthly rainfalls under SSP1-2.6, SSP2-4.5, and SSP5-8.5 scenarios for future periods 2021–2050 and 2051–2080 and with respect to baseline period of 1976–2005

future period and 20% under SSP1-2.6 for the far future period. SSP5-8.5 indicates a higher rainfall increase than SSP1-2.6 and SSP2-4.5 from August to November for two future periods, with increments ranging between 11.1 and 23% for the near future period and 19.4% to 36.1% for the far future period. The projected future rainfall under SSP1-2.6 and SSP2-4.5 seems to be higher than SSP5-8.5 from January to July and December, but SSP5-8.5 seems to be higher than July to November SSP1 and SSP2.

In Malaysia, lower rainfall is observed normally during February to July compared to the remaining months of the year. Therefore the result predicted that more dry days would appear in these months in the future. The CMIP6 multi-GCM ensemble predicted mean monthly rainfalls show significant increasing trends in February, July to December in both future periods. Greater

increase in the mean monthly rainfall is predicted under SSP5-8.5 scenario compared to SSP1-2.6 and SSP2-4.5 scenarios during 2021–2050 and 2051–2080. In general, the model shows that most scenarios predict the increasing trend of the mean monthly rainfall with only a few months project negative changes in April and May.

Figure 8 illustrates cumulative frequency distribution for CMIP6 multi-GCM ensemble mean monthly projected rainfalls of Kurau River Basin for 2021–2050 and 2051–2080. The projected output is more likely to increase for all three SSP scenarios in the future. It is clearly evident that the mean monthly rainfall pattern is expected to change in the future compared to the baseline period of 1976–2005. The future projection reveals increasing trends in most of the months with decreasing only a few months of the year. The projected monthly

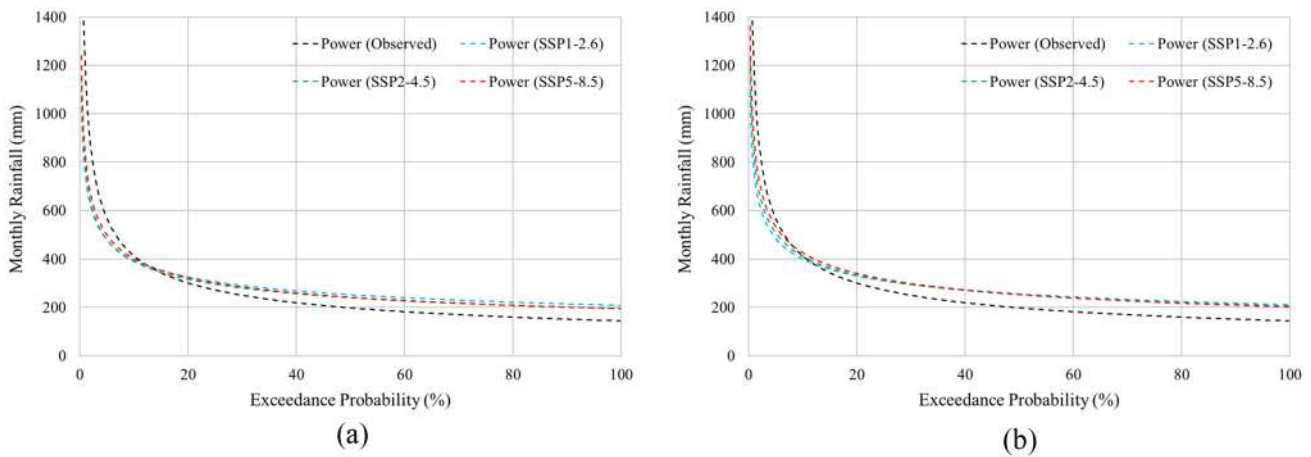


Fig. 8 Cumulative frequency distribution of the projected multi-GCM ensemble mean monthly rainfall at Kurau River Basin of observed (1976–2005) and future periods; **a** 2021–2051 and **b** 2051–2080

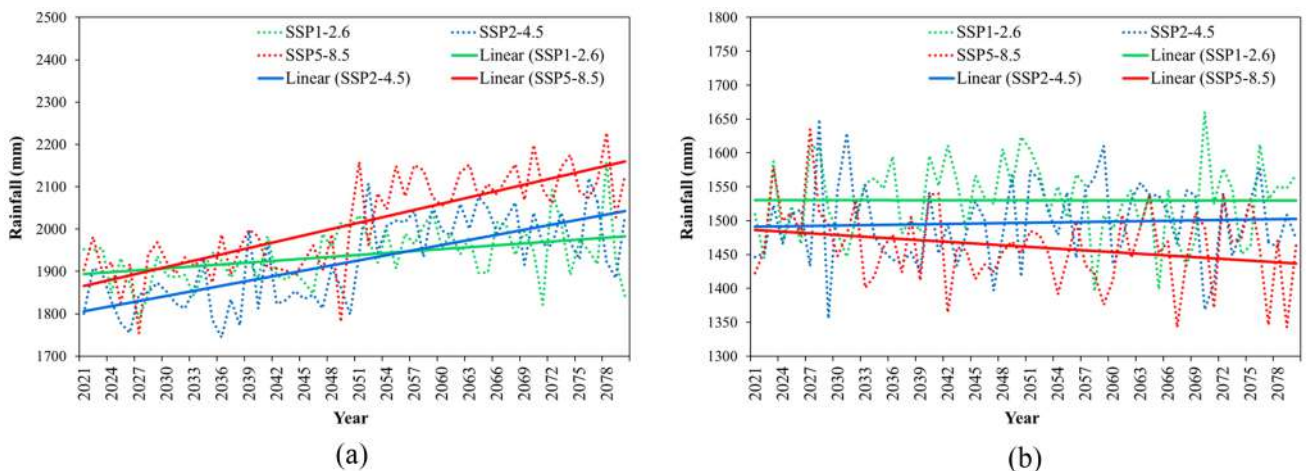


Fig. 9 Projected ensemble annual rainfall under SSP1-2.6, SSP2-4.5, and SSP5-8.5 scenarios over 2021–2080 for **a** main-season and **b** off-season

rainfall will be range between 200 and 400 mm with a higher possibility of around 200 mm.

The impact of climate change will affect agricultural water management by causing excess rainfall, especially during the main-season, as illustrated in Fig. 9. The figure reveals that the main (wet)-season will become wetter under all SSP scenarios, with SSP5-8.5 being the highest. While during the off-season the amount of rainfall is much less compared to the main-season, with SSP5-8.5 being the worst and significantly decreasing toward 2080. The result is supported by the statistical analysis displayed in Table 5, where the future period is expected to face longer wet and dry spells with rainy days increasing during the main-season, and decreasing during the off-season except for SSP1-2.6. Wet and dry spells mentioned in this study are the maximum consecutive wet or dry days in a month. Dry spell series have often been given attention when

dealing with agriculture as they can adversely impact cultivation and production. These changes will alter the hydrologic response on the basin, affect the inflows to the reservoir, and affect the two planting seasons of rice cultivation every year. Rice cultivation practices involve the uniform application of 100 mm irrigation water around 7 to 10 days to maintain the standing water depth on rice system, where this volume is depleted in assuming daily evapotranspiration and seepage occur 3–4 and 2–3 mm, respectively [46]. The portion of rainfall stored in the root zone after the rest evaporated from the earth's surface and used for rice crops is called effective rainfall.

Effective rainfall is a crucial component in assessing optimum rice irrigation water requirements. Future effective rainfall will follow a trend similar to projected rainfall, as portrayed in Fig. 10. Higher rainfall will have higher effective rainfall, thus reducing the irrigation supply from

Table 5 Summary of monthly statistical analysis in rainfall parameters for baseline (1976–2005) and future scenarios (2021–2080) with percent change from baseline

Statistics analysis	Baseline	SSP1-2.6	SSP2-4.5	SSP5-8.5
Effective rainfall (main-season)	839 mm	904 mm (8%)	891 mm (6%)	918 mm (9%)
Effective rainfall (off-season)	771 mm	800 mm (3%)	785 mm (2%)	793 mm (3%)
Rainy days (main-season)	19.06	19.50 (2%)	19.70 (3%)	19.55 (3%)
Rainy days (off-season)	17.35	17.65 (2%)	17.26 (–1%)	16.97 (–2%)
Wet-spell length (days)	4.13	4.65 (12%)	4.43 (7%)	4.15 (0.5%)
Dry-spell length (days)	3.12	3.21 (3%)	3.31 (6%)	3.14 (0.6%)

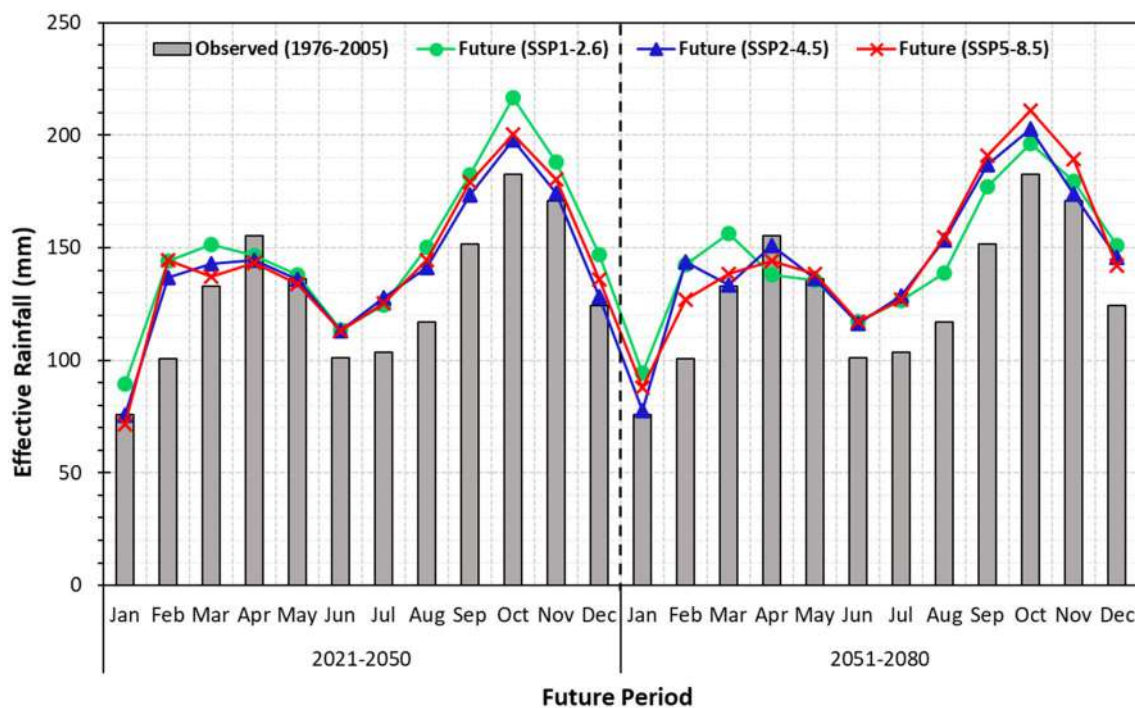


Fig. 10 Projected ensemble mean monthly effective rainfalls under SSP1-2.6, SSP2-4.5, and SSP5-8.5 scenarios for future periods 2021–2050 and 2051–2080 and with respect to baseline period of 1976–2005

the reservoir to the rice field and vice-versa. Projected effective rainfall for SSP1-2.6, SSP2-4.5, and SSP5-8.5 is predicted to increase about 15.8%, 12.0%, and 12.7%, respectively, with SSP1-2.6, has the highest increases followed by SSP5-8.5 and SSP2-4.5. Furthermore, the SSP1-2.6 illustrates that 2021–2050 have higher mean monthly effective rainfall compared to SSP2-4.5 and SSP5-8.5, but during 2051–2080 it is predicted to be lower than SSP2-4.5 and SSP5-8.5. February is predicted to have the most significant mean monthly effective rainfall increase for SSP1-2.6, SSP2-4.5, and SSP5-8.5 with values 43.3%, 36.1%, and 43.6% for 2021–2050 and 41.7%, 43.0%, and 26.4% for 2051–2080, respectively.

Based on the findings, there is a possibility of floods occurring during the main rice-growing season and heat stress during the off-season. Therefore the results suggest that a higher projection of future rainfall during the main (wet) season of planting period months (August–July) stored in the reservoir should be well managed and optimized. The aim is to reduce wastage of water supply to the rice field to cope with the possibility of water shortage during off (dry) season of planting period months (February–July) due to possible longer dry spells and less number of rainy days.

4 Conclusion

Rainfall is a driving element to ensure the sustainability of rice cultivation and production. Therefore, awareness of how the future rainfall pattern is likely to change is mandatory within the rice-growing areas in Malaysia. This study reveals the impact of climate change on future rainfall by an ensemble of five GCMs under CMIP6 and three SSP narratives (SSP1-2.6, SSP2-4.5, and SSP5-8.5) at a grid point considering the rice-growing area of Kerian, Perak, Malaysia. The stochastic rainfall generator model (Markov-chain and Gamma distribution) combined with the change factor method is adopted to statistically downscale and simulate future rainfall for Kurau River Basin, the water source of the Kerian rice field. The selected technique provides satisfactory performance to reproduce observed data and downscaled multi-GCM outputs to establish future rainfall changes under different scenarios. However, the application of this method is not enough to capture extreme rainfall and drought events. As a recommendation, for these advanced studies, it is best to consider multi states and higher-order formulation.

The results obtained for each downscaled rainfall under GCM are variable, giving the uncertainties in future rainfall changes. Therefore it is recommended to use more GCM models to bridge this gap. Despite that, the projected pattern agrees with the direction of changes in the rainfall

scenario for the study area. The CMIP6 multi-GCM ensemble models show that most scenarios predict the increasing trend of the mean monthly rainfall with only April and May project decrease changes occurring in off (dry) season. The future monthly patterns for 2051–2080 show a significant increasing trend during main (wet) season compared to the near future period (2021–2050). Generally, future annual rainfall is projected to increase significantly during the main-season period under all SSPs, but the changes are insignificant during the off-season except under SSP5-8.5, which decreases toward the end of the period.

The future monthly effective rainfall will have a similar trend pattern as projected future rainfall from CMIP6 multi-GCM ensemble. Effective rainfall is an important parameter in assessing optimum rice irrigation water requirements. Based on the projected rainfall results, the rice-growing area is expected to experience an increase of effective rainfall for both planting seasons and significantly during the main-season. The rice-growing area will become wet during off (dry) season and wetter during main (wet) season. This finding is important for rice farmers and water managers to make decisions for future water management to secure the rice sector of the area. However, the projected changes in rainfall on the river basin require further study before concluding its impact consequences on the rice field.

Acknowledgements The authors would like to thank the Ministry of Higher Education (MOHE), Universiti Putra Malaysia (UPM), and Universiti Teknologi Malaysia (UTM) for supporting this research work. The authors are grateful to the Department of Irrigation and Drainage (DID) for providing gauged rainfall data for the study.

Authors' contributions MNMA carried out the study, analyzed the data, and drafted the manuscript, SH supervised and conceptualized the manuscript, and MKR supervised and reviewed the manuscript.

Funding The authors have not disclosed any funding

Availability of data and materials The data sets of gauged rainfall of Kurau River Basin, Perak, Malaysia that support the findings of this study can be requested from the Department of Irrigation and Drainage (DID) or the corresponding author upon reasonable request.

Declarations

Conflict of interest The authors declare no competing interests.

Open Access This article is licensed under a Creative Commons Attribution 4.0 International License, which permits use, sharing, adaptation, distribution and reproduction in any medium or format, as long as you give appropriate credit to the original author(s) and the source, provide a link to the Creative Commons licence, and indicate if changes were made. The images or other third party material in this article are included in the article's Creative Commons licence, unless indicated otherwise in a credit line to the material. If material is not

included in the article's Creative Commons licence and your intended use is not permitted by statutory regulation or exceeds the permitted use, you will need to obtain permission directly from the copyright holder. To view a copy of this licence, visit <http://creativecommons.org/licenses/by/4.0/>.

References

1. Kwan MS, Tanggang FT, Juneng L (2011) Projected changes of future climate extremes in Malaysia. National Symposium on Climate Change Adaptation. *Sains Malays* 42:1051–1058
2. Tang KHD (2019) Climate change in Malaysia: trends, contributors, impacts, mitigation and adaptations. *Sci Total Environ* 650:1858–1871. <https://doi.org/10.1016/j.scitotenv.2018.09.316>
3. IPCC (2013) Climate change 2013: the physical science basis. Contribution of working group I to the fifth assessment report of the intergovernmental panel on climate change. Cambridge University Press, Cambridge
4. Nakicenovic N, Alcamo J, Grubler A et al (2000) Special report on emissions scenarios (SRES), a special report of working group III of the intergovernmental panel on climate change. Cambridge University Press, Cambridge
5. Hassan Z, Harun S, Malek MA (2012) Application of ANNs model with the SDSM for the hydrological trend prediction in the sub-catchment of Kurau River, Malaysia. *J Environ Sci Eng* 1:577–585
6. Matthews RB, Kropff MJ, Horie T, Bachelet D (1997) Simulating the impact of climate change on rice production in asia and evaluating options for adaptation. *Agric Syst* 54:399–425. [https://doi.org/10.1016/S0308-521X\(95\)00060-1](https://doi.org/10.1016/S0308-521X(95)00060-1)
7. Lee TS, Haque MA, Najim MMM (2005) Scheduling the cropping calendar in wet-seeded rice schemes in Malaysia. *Agric Water Manag* 71:71–84. <https://doi.org/10.1016/j.agwat.2004.06.007>
8. Dlamini NS, Rowshon MK, Saha U et al (2015) Simulation of future daily rainfall scenario using stochastic rainfall generator for a rice-growing irrigation scheme in Malaysia. *Asian J Appl Sci* 03:492–506
9. Han J, Miao C, Duan Q et al (2020) Variations in start date, end date, frequency and intensity of yearly temperature extremes across China during the period 1961–2017. *Environ Res Lett* 15:045007. <https://doi.org/10.1088/1748-9326/ab7390>
10. Zarrin A, Dadashi-Roudbari A (2021) Projection of future extreme precipitation in Iran based on CMIP6 multi-model ensemble. *Theor Appl Climatol* 144:643–660. <https://doi.org/10.1007/s00704-021-03568-2>
11. Ahmadi H, Rostami N, Dadashi-roudbari A (2020) Projected climate change in the Karkheh Basin, Iran, based on CORDEX models. *Theor Appl Climatol* 142:661–673. <https://doi.org/10.1007/s00704-020-03335-9>
12. Abbasian M, Moghim S, Abrishamchi A (2019) Performance of the general circulation models in simulating temperature and precipitation over Iran. *Theor Appl Climatol* 135:1465–1483. <https://doi.org/10.1007/s00704-018-2456-y>
13. Taylor KE, Stouffer RJ, Meehl GA (2012) An overview of CMIP5 and the experiment design. *Bull Am Meteorol Soc* 93:485–498. <https://doi.org/10.1175/BAMS-D-11-00094.1>
14. Riahi K, van Vuuren DP, Kriegler E et al (2017) The Shared Socio-economic Pathways and their energy, land use, and greenhouse gas emissions implications: an overview. *Glob Environ Change* 42:153–168. <https://doi.org/10.1016/j.gloenvcha.2016.05.009>
15. Moss RH, Edmonds JA, Hibbard KA et al (2010) The next generation of scenarios for climate change research and assessment. *Nature* 463:747–756. <https://doi.org/10.1038/nature08823>
16. Eyring V, Bony S, Meehl GA et al (2016) Overview of the Coupled Model Intercomparison Project Phase 6 (CMIP6) experimental design and organization. *Geosci Model Dev* 9:1937–1958. <https://doi.org/10.5194/gmd-9-1937-2016>
17. Rowshon MK, Dlamini NS, Mojid MA et al (2019) Modeling climate-smart decision support system (CSDSS) for analyzing water demand of a large-scale rice irrigation scheme. *Agric Water Manag* 216:138–152. <https://doi.org/10.1016/j.agwat.2019.01.002>
18. Sidhu RK, Kumar R, Rana PS (2020) Machine learning based crop water demand forecasting using minimum climatological data. *Multimed Tools Appl* 79:13109–13124. <https://doi.org/10.1007/s11042-019-08533-w>
19. Holzkämper A, Calanca P, Fuhrer J (2012) Statistical crop models: Predicting the effects of temperature and precipitation changes. *Clim Res* 51:11–21. <https://doi.org/10.3354/cr01057>
20. Wilks DS (1992) Adapting stochastic weather generation algorithms for climate change studies. *Clim Change* 22:67–84. <https://doi.org/10.1007/BF00143344>
21. Richardson CW (1981) Stochastic modelling of daily precipitation, temperature and solar radiation. *Water Resour Res* 17:182–190. <https://doi.org/10.1029/WR017i001p00182>
22. Wilby RL (1999) The weather generation game: A review of stochastic weather models. *Prog Phys Geogr* 23:329–357. <https://doi.org/10.1177/030913339902300302>
23. Fadhil RM, Rowshon MK, Ahmad D et al (2017) A stochastic rainfall generator model for simulation of daily rainfall events in Kurau catchment: model testing. *Acta Hortic* 1152:1–10. <https://doi.org/10.17660/ActaHortic.2017.1152.1>
24. Liu H, Chen J, Zhang XC et al (2020) A Markov chain-based bias correction method for simulating the temporal sequence of daily precipitation. *Atmosphere (Basel)*. <https://doi.org/10.3390/atmos11010109>
25. Adib MNM, Rowshon MK, Mojid MA, Habibu I (2020) Projected streamflow in the Kurau River Basin of Western Malaysia under future climate scenarios. *Sci Rep* 10:8336. <https://doi.org/10.1038/s41598-020-65114-w>
26. Tan ML, Ficklin DL, Ibrahim AL, Yusop Z (2014) Impacts and uncertainties of climate change on streamflow of the johor River Basin, Malaysia using a cmip5 general circulation model ensemble. *J Water Clim Change* 5:676–695. <https://doi.org/10.2166/wcc.2014.020>
27. Hussain M, Yusof KW, Mustafa MR et al (2017) Projected changes in temperature and precipitation in Sarawak State of Malaysia for selected CMIP5 climate scenarios. *Int J Sustain Dev Plan* 12:1299–1311. <https://doi.org/10.2495/SDP-V12-N8-1299-1311>
28. Tan ML, Liang J, Samat N et al (2021) Hydrological extremes and responses to climate change in the Kelantan River Basin, Malaysia, based on the CMIP6 highresmip experiments. *Water (Switzerland)* 13:1472. <https://doi.org/10.3390/w13111472>
29. Wan Zin WZ, Jamaludin S, Deni SM, Jemain AA (2010) Recent changes in extreme rainfall events in Peninsular Malaysia: 1971–2005. *Theor Appl Climatol* 99:303–314. <https://doi.org/10.1007/s00704-009-0141-x>
30. Syafrina AH, Zalina MD, Juneng L (2015) Historical trend of hourly extreme rainfall in Peninsular Malaysia. *Theor Appl Climatol* 120:259–285. <https://doi.org/10.1007/s00704-014-1145-8>
31. Suhaila J, Deni SM, Zawiah Zin WAN, Jemain AA (2010) Trends in Peninsular Malaysia rainfall data during the southwest monsoon and northeast monsoon seasons: 1975–2004. *Sains Malays* 39:533–542

32. Swart NC, Cole JNS, Kharin VV et al (2019) The Canadian earth system model version 5 (CanESM5.0.3). *Geosci Model Dev* 12:4823–4873. <https://doi.org/10.5194/gmd-12-4823-2019>
33. Mauritsen T, Bader J, Becker T et al (2019) Developments in the MPI-M earth system model version 1.2 (MPI-ESM1.2) and its response to increasing CO₂. *J Adv Model Earth Syst* 11:998–1038. <https://doi.org/10.1029/2018MS001400>
34. Yukimoto S, Kawai H, Koshiro T et al (2019) The meteorological research institute Earth system model version 2.0, MRI-ESM2.0: description and basic evaluation of the physical component. *J Meteorol Soc Jpn* 97:931–965. <https://doi.org/10.2151/jmsj.2019-051>
35. Cao J, Wang B, Yang YM et al (2018) The NUIST earth system model (NESM) version 3: description and preliminary evaluation. *Geosci Model Dev* 11:2975–2993. <https://doi.org/10.5194/gmd-11-2975-2018>
36. Seland Ø, Bentsen M, Olivie D et al (2020) Overview of the Norwegian Earth System Model (NorESM2) and key climate response of CMIP6 DECK, historical, and scenario simulations. *Geosci Model Dev* 13:6165–6200. <https://doi.org/10.5194/gmd-13-6165-2020>
37. Dlamini NS, Rowshon MK, Saha U et al (2015) Developing and calibrating a stochastic rainfall generator model for simulating daily rainfall by Markov chain approach. *J Teknol* 76:13–19. <https://doi.org/10.11113/jt.v76.5946>
38. Liu H, Sun Y, Yin X et al (2020) A reservoir operation method that accounts for different inflow forecast uncertainties in different hydrological periods. *J Clean Prod* 256:120471. <https://doi.org/10.1016/j.jclepro.2020.120471>
39. Sadiq N (2014) Stochastic modelling of the daily rainfall frequency and amount. *Arab J Sci Eng* 39:5691–5702. <https://doi.org/10.1007/s13369-014-1132-5>
40. Zhou Y, Shang Y, Li J, Tang Q (2017) Stochastic long time series rainfall generation method. In: International low impact development conference China 2016—ASCE, pp 92–99
41. Deni SM, Suhaila J, Wan Zin WZ, Jemain AA (2010) Spatial trends of dry spells over Peninsular Malaysia during monsoon seasons. *Theor Appl Climatol* 99:357–371. <https://doi.org/10.1007/s00704-009-0147-4>
42. Fatichi S, Ivanov VY, Caporali E (2011) Simulation of future climate scenarios with a weather generator. *Adv Water Resour* 34:448–467. <https://doi.org/10.1016/j.advwatres.2010.12.013>
43. Suhaila J, Jemain AA (2009) Investigating the impacts of adjoining wet days on the distribution of daily rainfall amounts in Peninsular Malaysia. *J Hydrol* 368:17–25. <https://doi.org/10.1016/j.jhydrol.2009.01.022>
44. Suhaila J, Jemain AA (2009) A comparison of the rainfall patterns between stations on the East and the West coasts of Peninsular Malaysia using the smoothing model of rainfall amounts. *Meteorol Appl* 16:391–401. <https://doi.org/10.1002/met>
45. Wilks DS, Wilby RL (1999) The weather generation game: a review of stochastic weather models. *Prog Phys Geogr* 23:329–357. <https://doi.org/10.1191/030913399666525256>
46. Lee TS, Haque MA, Huang YF (2006) Modeling water balance components in rice field irrigation. *Inst Eng Malays* 67:22–25

Publisher's Note Springer Nature remains neutral with regard to jurisdictional claims in published maps and institutional affiliations.